Advances in Engineering Software 175 (2023) 103286

Contents lists available at ScienceDirect

Advances in Engineering Software

journal homepage: www.elsevier.com/locate/advengsoft

Imposing displacements in implicit direct time integration & a patch test

Gunwoo Noh [a,*], Klaus-Jürgen Bathe [b]

[a] Korea University, Seoul 02841, Republic of Korea
[b] Massachusetts Institute of Technology, Cambridge, MA 02139, USA

ARTICLE INFO

Keywords:
Transient dynamics
Implicit time integration
Imposing displacements
Trapezoidal Rule
Bathe method
Stability and accuracy

ABSTRACT

We consider the transient analysis of finite element models when an implicit direct time integration scheme is used and focus on the accuracy of the response solution when time varying nodal displacements are imposed. The solutions of such problems are abundantly sought in engineering practice. We analyze the performance of the widely used Trapezoidal Rule, a specific case of Newmark time integration, and the performance of the Bathe method. The theoretical results show that the Trapezoidal Rule is *unstable* and this instability becomes more pronounced as the time step size for solution is *decreased*, whereas the Bathe method is stable. We illustrate these theoretical findings in the transient analyses of some finite element models. These investigations lead us to define a "patch test" useful for the general evaluation of direct time integration schemes.

1. Introduction

The finite element method is now commonly used for the solution of physical problems. Among the many simulations performed in engineering and the sciences, transient dynamic solutions can be important. For such solutions, a direct implicit time integration is frequently performed with an unconditionally stable time integration scheme [1–3].

An alternative approach is to use an explicit direct time integration scheme, but then a stability limit on the time step size needs to be satisfied. Mode superposition can also be employed but is largely restricted to linear analysis, although local nonlinearities can be included [3].

The key is to use in the direct time integration an effective solution scheme. We call the integration "direct" because the solution is performed *directly* using the governing finite element equations without a prior transformation to a new basis. Such a transformation is applied in the solution using mode superposition. Therefore, direct integration can be performed in linear and nonlinear analyses.

However, to analyze a direct integration scheme we consider linear analysis and think of the superposition of modal responses during the time integration – only conceptually because the frequencies and mode shapes are of course not evaluated. Hence, we can consider the response of a single linear degree of freedom system of frequency ω and damping ξ, which both can take on different values, with an applied initial displacement, initial velocity and perhaps load to measure the accuracy achieved.

A very widely used implicit time integration scheme is the Trapezoidal Rule (TR) of the Newmark method, which is obtained by setting the two Newmark method parameters δ and α to $\delta = \frac{1}{2}$ and $\alpha = \frac{1}{4}$ [4]. This scheme is unconditionally stable, easy to implement, can be used in linear and nonlinear analyses, and over decades has proven successful in many applications.

However, the TR has also major shortcomings. Hence an analyst using the Newmark method may for this reason employ other values for the parameters δ and α, but then different shortcomings are encountered, most notably that the accuracy of the solution scheme is not good [5–9].

The important properties commonly sought in an implicit time integration scheme are:

- The method should be unconditionally stable, which means in simple terms that the solution, hence also any errors like due to round-off, will not "blow up" for any time step size used.
- The method should not give an "overshoot" in the solution, which means in simple terms that when a problem is solved with initial conditions only, the solution should not give results larger than the initial conditions. A typical case to consider is ${}^0u = 1.0,\ {}^0\dot{u} = 0,\ {}^0\ddot{u} = -\omega^2$ where u denotes the displacement, an over dot means time derivative and the left superscript indicates the time considered.
- The method should contain numerical damping, which means in simple terms that for a large time step Δt to period ratio, $\Delta t/T$, where

* Corresponding author.
E-mail address: gunwoonoh@korea.ac.kr (G. Noh).

https://doi.org/10.1016/j.advengsoft.2022.103286
Received 19 June 2022; Received in revised form 21 August 2022; Accepted 7 September 2022
Available online 21 November 2022

T denotes the natural period, the numerical solution will correspond to a very damped numerical response.

The first two properties are relatively easy to satisfy. The third property can also easily be satisfied – except when we look for the "best" accuracy in the solution.

An ideal numerical damping in implicit direct time integration shows little amplitude decay for a time step to period ratio smaller than 1/3 and for greater ratios the amplitude decay rapidly grows. Namely, it is reasonable to use 3 time steps per period for the time integration in order to obtain an accurate solution in that period (and those of lower frequencies) but for a larger time step any calculated response will likely be inaccurate and is better rapidly damped out. This property is important to obtain solution accuracy in the frequencies and modes that are excited and not have that response polluted with a "spurious" response.

To test for these three properties, we refer to some references of the many available, see Refs. [1–19]. The above conditions of unconditional stability, no-overshoot and the need for numerical damping are well-known and have been amply analyzed and numerally demonstrated [1–19]. In Ref. [19], in particular, a two-degree of freedom model of a soft and a very stiff spring is used to evaluate the solution accuracy obtained when no numerical damping is present and appropriate numerical damping is used. Such conditions of flexible and very stiff behavior are frequently encountered in practical finite element analyses, like of structures containing thin shells, flexible and stiff beams, or modeled with meshes using large and very small, narrow finite elements.

We may think of the tests for the three above conditions with the test used in Refs. [9,17,20,21] – a two-degree of freedom model of a soft and a very stiff spring – as part of a "patch test" for time integration schemes. The patch test for spatial discretizations, see e.g., Refs. [3,22], is well known and abundantly used in evaluating the overall effectiveness of finite elements, but here we think of a patch test to evaluate the overall effectiveness of a time integration method.

Our objective in this paper is to discuss a fourth important property for an effective time integration scheme and to introduce an important addition to be incorporated in the "time integration patch test".

An effective time integration scheme should also give an accurate solution when displacements are imposed, not just forces. Displacements might be imposed as a function of time at certain nodes of a finite element model, like in the transient analyses of machinery equipment, in the response solutions of bridges, the dynamic simulations of motor cars, and so on. In each such case, an accurate response solution is expected. Hence we should also test whether a time integration scheme can be used effectively when displacements are imposed.

The impetus for us to write this paper was that we observed – to our surprise – that the widely-used Trapezoidal Rule (TR) predicted an unreasonable response in engineering practice when time-varying displacements are imposed[1]. When forces are applied, the TR is of course known to give spurious response solutions if the time step is too large and to give an accurate solution if the time step is small enough. However, here we consider that time varying displacements are imposed and find that the *spurious response increases as the time step size decreases*. This observation is clearly important and needs a deeper understanding and hence a theoretical analysis.

In the following, we first present our theoretical results of an analysis when a displacement is imposed on a single degree of freedom system and then on a multi-degree of freedom system. We consider the TR and the standard Bathe method [23,24]. This discussion includes the response obtained analytically for the velocity and acceleration. We then illustrate these theoretical observations in the example solutions of a simple structural dynamics problem using one linear finite element and a two-dimensional wave propagation problem. Finally, we give our concluding remarks.

2. The governing equations with prescribed displacements and their analyses

As mentioned above already, the Trapezoidal Rule of the Newmark time integration scheme has been abundantly studied and is widely used in implicit time integration solutions. We consider this time integration scheme first.

Another time integration scheme, much more recently proposed is the Bathe method [23,24], which we consider thereafter.

In both cases we want to solve the following n equations

$$\mathbf{M}\ddot{\mathbf{U}} + \mathbf{C}\dot{\mathbf{U}} + \mathbf{K}\mathbf{U} = \mathbf{F} \tag{1}$$

with the initial conditions

$$\mathbf{U}_{(t=0)} = {}^0\mathbf{U}; \quad \dot{\mathbf{U}}_{(t=0)} = {}^0\dot{\mathbf{U}} \tag{2}$$

where in Eq. (1) the matrices **M, C** and **K** are the mass, damping and stiffness matrices, U is the vector of nodal displacements (possibly also including rotations), an over dot denotes time derivative, and in Eq. (2), the left superscript denotes the time considered. In general, the number of finite element equilibrium equations (n) considered in Eq. (1) can be small or large (100,000 or even larger). Hence the direct time integration has to be as effective as possible.

As mentioned above, although we want to solve Eqs. (1) and (2), for the analysis of a time integration scheme we consider a single degree of freedom system representing all n modal responses

$$\ddot{u} + 2\xi\omega\dot{u} + \omega^2 u = f \tag{3}$$

which represents Eq. (1) using a unit mass, the damping $2\xi\omega$, with ξ the critical damping ratio, and the stiffness ω^2. To cover all possible cases of finite element equations, we consider $0 \le \omega \le \infty$. The initial displacement and velocity are prescribed as in Eq. (2).

In earlier studies of time integration schemes, emphasis is placed on the stability and accuracy of the integration for initial conditions and externally applied forces. The spectral radius, amplitude decay and period elongation are used to establish the accuracy characteristics of a scheme [3]. We now consider the imposition of given displacements.

In the following sections, we first identify the errors that occur when a displacement is imposed in Eq. (3) and then study how those errors propagate to other degrees of freedom in the finite element model.

2.1. The Trapezoidal Rule

Considering a typical degree-of-freedom subjected to a prescribed displacement, we use in the Newmark method [4]

$$\begin{aligned} {}^{t+\Delta t}\ddot{u}_p &= a_0\left({}^{t+\Delta t}u_p - {}^t u_p\right) - a_2\,{}^t\dot{u}_p - a_3\,{}^t\ddot{u}_p \\ {}^{t+\Delta t}\dot{u}_p &= {}^t\dot{u}_p + a_6\,{}^t\ddot{u}_p + a_7\,{}^{t+\Delta t}\ddot{u}_p \end{aligned} \tag{4}$$

with

$$a_0 = \frac{1}{\alpha\Delta t^2}; \quad a_2 = \frac{1}{\alpha\Delta t}; \quad a_3 = \frac{1}{2\alpha} - 1; \quad a_6 = \Delta t(1-\delta); \quad a_7 = \delta\Delta t \tag{5}$$

where the subscript p on the solution variables signifies that we consider the solution at the "prescribed displacement".

Using Eqs. (4) and (5) we have

$${}^{t+\Delta t}\dot{u}_p = (1 - a_2 a_7)\,{}^t\dot{u}_p + (a_6 - a_3 a_7)\,{}^t\ddot{u}_p + a_6 a_7\left({}^{t+\Delta t}u_p - {}^t u_p\right) \tag{6}$$

[1] Dr. T. Sussman and Dr. J. Walczak first mentioned this deficiency to us, see Acknowledgments.

To obtain the TR we use $\delta = \frac{1}{2}$, $\alpha = \frac{1}{4}$ and have

$$\begin{bmatrix} {}^{t+\Delta t}\dot{u}_p \\ {}^{t+\Delta t}\ddot{u}_p \end{bmatrix} = \begin{bmatrix} -1 & 0 \\ -\frac{4}{\Delta t} & -1 \end{bmatrix} \begin{bmatrix} {}^{t}\dot{u}_p \\ {}^{t}\ddot{u}_p \end{bmatrix} + \begin{bmatrix} \frac{2}{\Delta t}\left({}^{t+\Delta t}u_p - {}^{t}u_p\right) \\ \frac{4}{\Delta t^2}\left({}^{t+\Delta t}u_p - {}^{t}u_p\right) \end{bmatrix} \tag{7}$$

Since the displacements are prescribed, ${}^{t}u_p, {}^{t+\Delta t}u_p$ are known for all times, and the unknowns are the velocity and acceleration.

Since the eigenvalues of the coefficient matrix $\bar{\mathbf{A}}_{\mathrm{TR}}$

$$\bar{\mathbf{A}}_{\mathrm{TR}} = \begin{bmatrix} -1 & 0 \\ -\frac{4}{\Delta t} & -1 \end{bmatrix} \tag{8}$$

are $\lambda_1 = 1$, $\lambda_2 = -1$, the solution is only "borderline stable".

2.1.1. Velocity results

Considering the results for the velocity, we obtain from Eq. (7)

$${}^{t+\Delta t}\dot{u}_p = -{}^{t}\dot{u}_p + \frac{2}{\Delta t}\left({}^{t+\Delta t}u_p - {}^{t}u_p\right) \tag{9}$$

To understand how the errors evolve in the calculated velocity time history, we define

$${}^{t}\dot{r}_p = {}^{t}\dot{u}_p - \dot{u}_p(t) \tag{10}$$

where ${}^{t}\dot{r}_p$ is the "velocity residual error", that is, the difference between the calculated velocity ${}^{t}\dot{u}_p$ using the TR and the analytically exact velocity $\dot{u}_p(t)$. This residual error is not a round-off error, hence we use "$\dot{r}$" (r for residual) to denote it, and would even exist if we were to use an infinite precision computer. But in the following we will refer simply to the "error" without including the word "residual". Also, considering the superscript "t" we use ${}^{t}x$ and $x(t)$ to refer to the numerically computed value and the corresponding exact value of a solution variable x at time t, respectively.

From Eq. (10), we have

$${}^{t}\dot{u}_p = {}^{t}\dot{r}_p + \dot{u}_p(t) \tag{11}$$

Similarly

$${}^{t+\Delta t}\dot{u}_p = {}^{t+\Delta t}\dot{r}_p + \dot{u}_p(t+\Delta t) \tag{12}$$

and therefore Eq. (9) can be written as

$${}^{t+\Delta t}\dot{r}_p = -{}^{t}\dot{r}_p + \frac{2}{\Delta t}\left({}^{t+\Delta t}u_p - {}^{t}u_p\right) - \dot{u}_p(t) - \dot{u}_p(t+\Delta t) \tag{13}$$

We are interested in identifying how the error in the solution behaves as the time stepping proceeds when displacements are imposed, that is,

$${}^{t}u_p = u_p(t) \;\; ; \;\; {}^{t+\Delta t}u_p = u_p(t+\Delta t) \tag{14}$$

We next aim to eliminate the displacements and velocities in Eq. (13) to be only left with the velocity error and higher-order terms in Δt. For this purpose, we use a Taylor series expansion in Δt on the displacements in Eq. (13). We find that the velocities then cancel out and arrive at

$${}^{t+\Delta t}\dot{r}_p = -{}^{t}\dot{r}_p + O^{l}\left(\Delta t^2\right) \tag{15}$$

or after n steps

$${}^{n\Delta t}\dot{r}_p = (-1)^n\, {}^{0}\dot{r}_p + O^{g}\left(\Delta t^2\right) \tag{16}$$

with the superscript l and g on O signifying "local" and "global", respectively.

As expected, the result is simply that the numerical solutions ${}^{t}\dot{u}_p$, ${}^{t+\Delta t}\dot{u}_p$, in Eq. (9) are replaced by the errors ${}^{t}\dot{r}_p$, ${}^{t+\Delta t}\dot{r}_p$ plus the truncation error which for the velocities is $O(\Delta t^2)$ The propagation of the error is governed by the coefficient matrix $\bar{\mathbf{A}}_{\mathrm{TR}}$.

Eqs. (15) and (16) show that the leading term of the magnitude of the velocity error at any time point is not a function of time step size: therefore, the amplitude of the error is independent of the time step size used, both locally and globally. This observation also follows from the first row of the matrix $\bar{\mathbf{A}}_{\mathrm{TR}}$.

2.1.2. Acceleration results

We proceed as in Section 2.1.1 but now focus on the solution of the acceleration. From Eq. (7), we have

$${}^{t+\Delta t}\ddot{u}_p = -\frac{4}{\Delta t}{}^{t}\dot{u}_p - {}^{t}\ddot{u}_p + \frac{4}{\Delta t^2}\left({}^{t+\Delta t}u_p - {}^{t}u_p\right) \tag{17}$$

The error in acceleration is the difference between the acceleration computed by the TR ${}^{t}\ddot{u}_P$ and the exact acceleration $\ddot{u}_p(t)$

$${}^{t}\ddot{r}_p = {}^{t}\ddot{u}_p - \ddot{u}_p(t) \tag{18}$$

and similarly for the values at time $t + \Delta t$. Eq. (17) can then be written as

$${}^{t+\Delta t}\ddot{r}_p = -\frac{4}{\Delta t}{}^{t}\dot{r}_p - {}^{t}\ddot{r}_p + \frac{4}{\Delta t^2}\left({}^{t+\Delta t}u_p - {}^{t}u_p\right) - \frac{4}{\Delta t}\dot{u}_p(t) - \ddot{u}_p(t+\Delta t) - \ddot{u}_p(t) \tag{19}$$

Using Eq. (14) and proceeding as in the derivation of Eq. (15), again using the Taylor series in Δt on the displacements by which also the exact velocity and accelerations are eliminated, we obtain

$${}^{t+\Delta t}\ddot{r}_p = -\frac{4}{\Delta t}{}^{t}\dot{r}_p - {}^{t}\ddot{r}_p + O^{l}(\Delta t) \tag{20}$$

and with Eq. (16),

$${}^{n\Delta t}\ddot{r}_p = (-1)^n \frac{4n^0\dot{r}_p}{\Delta t} + (-1)^n\, {}^{0}\ddot{r}_p + O^{g}(\Delta t) \tag{21}$$

This result corresponds to the second row in the matrix $\bar{\mathbf{A}}_{\mathrm{TR}}$. Eq. (21) shows that the global error in acceleration at a specific time t depends on Δt^{-2}, since in Eq. (21) $n = t/\Delta t$.

2.2. The Bathe method

In this scheme the total time step is subdivided into two sub-steps. In the first publications of the method two equal time sub-steps were used [23,24]; thereafter the subdividing was generalized to not necessarily use equal sub-steps [9,17]. The calculations for conditions within the time step can be considered simply to be part of the evaluation of the conditions to reach from time t to time $t + \Delta t$.

In the first sub-step the Bathe method uses the TR and in the second sub-step, the procedure uses the three-point Euler backward scheme.

Using equal sub-steps we obtain for the first sub-step, with ${}^{t}u_p$, ${}^{t+\Delta t/2}u_p$ known and simply using Eq. (7)

$$\begin{bmatrix} {}^{t+\frac{\Delta t}{2}}\dot{u}_p \\ {}^{t+\frac{\Delta t}{2}}\ddot{u}_p \end{bmatrix} = \begin{bmatrix} -1 & 0 \\ -\frac{8}{\Delta t} & -1 \end{bmatrix} \begin{bmatrix} {}^{t}\dot{u}_p \\ {}^{t}\ddot{u}_p \end{bmatrix} + \begin{bmatrix} \frac{4}{\Delta t}\left({}^{t+\frac{\Delta t}{2}}u_p - {}^{t}u_p\right) \\ \frac{16}{(\Delta t)^2}\left({}^{t+\frac{\Delta t}{2}}u_p - {}^{t}u_p\right) \end{bmatrix} \tag{22}$$

In the second sub-step, the scheme then uses

$${}^{t+\Delta t}\dot{u}_p = \frac{1}{\Delta t}{}^{t}u_p - \frac{4}{\Delta t}{}^{t+\frac{\Delta t}{2}}u_p + \frac{3}{\Delta t}{}^{t+\Delta t}u_p \tag{23}$$

and

$${}^{t+\Delta t}\ddot{u}_p = \frac{1}{\Delta t}{}^{t}\dot{u}_p - \frac{4}{\Delta t}{}^{t+\frac{\Delta t}{2}}\dot{u}_p + \frac{3}{\Delta t}{}^{t+\Delta t}\dot{u}_p \tag{24}$$

We want an equation like Eq. (22) but now for the full step Δt. Using the first row of Eq. (22) we have

$$ {}^{t+\frac{\Delta t}{2}}\dot{u}_p = -{}^{t}\dot{u}_p + \frac{4}{\Delta t}\left({}^{t+\frac{\Delta t}{2}}u_p - {}^{t}u_p\right) \tag{25}$$

Substituting into Eq. (24), we have

$$ {}^{t+\Delta t}\ddot{u}_p = \left\{ -{}^{t}\dot{u}_p + \frac{4}{\Delta t}\left({}^{t+\frac{\Delta t}{2}}u_p - {}^{t}u_p\right)\right\}\left(-\frac{4}{\Delta t}\right) + \frac{1}{\Delta t}{}^{t}\dot{u}_p + \frac{3}{\Delta t}{}^{t+\Delta t}\dot{u}_p \tag{26}$$

which then gives, using also Eq. (23)

$$ {}^{t+\Delta t}\ddot{u}_p = \left(\frac{5}{\Delta t}\right){}^{t}\dot{u}_p - \frac{16}{(\Delta t)^2}\left({}^{t+\frac{\Delta t}{2}}u_p - {}^{t}u_p\right) + \frac{3}{\Delta t}\left(\frac{1}{\Delta t}{}^{t}u_p - \frac{4}{\Delta t}{}^{t+\frac{\Delta t}{2}}u_p + \frac{3}{\Delta t}{}^{t+\Delta t}u_p\right) \tag{27}$$

Now we can write in matrix form:

$$ \begin{bmatrix} {}^{t+\Delta t}\dot{u}_p \\ {}^{t+\Delta t}\ddot{u}_p \end{bmatrix} = \begin{bmatrix} 0 & 0 \\ \frac{5}{\Delta t} & 0 \end{bmatrix} \begin{bmatrix} {}^{t}\dot{u}_p \\ {}^{t}\ddot{u}_p \end{bmatrix} + \begin{bmatrix} \frac{1}{\Delta t}{}^{t}u_p - \frac{4}{\Delta t}{}^{t+\frac{\Delta t}{2}}u_p + \frac{3}{\Delta t}{}^{t+\Delta t}u_p \\ -\frac{16}{(\Delta t)^2}\left({}^{t+\frac{\Delta t}{2}}u_p - {}^{t}u_p\right) + \frac{3}{\Delta t}\left(\frac{1}{\Delta t}{}^{t}u_p - \frac{4}{\Delta t}{}^{t+\frac{\Delta t}{2}}u_p + \frac{3}{\Delta t}{}^{t+\Delta t}u_p\right) \end{bmatrix} \tag{28}$$

Let

$$ \bar{\mathbf{A}}_{\mathrm{BM}} = \begin{bmatrix} 0 & 0 \\ \frac{5}{\Delta t} & 0 \end{bmatrix} \tag{29}$$

The eigenvalues of $\bar{\mathbf{A}}_{\mathrm{BM}}$ are $\lambda_1 = \lambda_2 = 0$ which makes the scheme very stable.

2.2.1. Velocity results

Using the results for the velocity from Eqs. (28) and (23), we obtain the velocity error at time $t+\Delta t$, that is ${}^{t+\Delta t}\dot{r}_p = {}^{t+\Delta t}\dot{u}_p - \dot{u}_p(t+\Delta t)$, as

$$ {}^{t+\Delta t}\dot{r}_p = \frac{1}{\Delta t}{}^{t}u_p - \frac{4}{\Delta t}{}^{t+\frac{\Delta t}{2}}u_p + \frac{3}{\Delta t}{}^{t+\Delta t}u_p - \dot{u}_p(t+\Delta t) \tag{30}$$

With the conditions of prescribed displacements for all time points, Eq. (14) and ${}^{t+\frac{\Delta t}{2}}u_p = u_p\left(t+\frac{\Delta t}{2}\right)$, and the Taylor series expansions, the velocity error reduces to

$$ {}^{t+\Delta t}\dot{r}_p = O^{l}\left(\Delta t^2\right) \tag{31}$$

which is the truncation error of the Euler 3-point backward rule in Eq. (23).

Of course, we expect from the eigenvalue of $\bar{\mathbf{A}}_{\mathrm{BM}}$ that the error at time t does not propagate to time $t+\Delta t$: the errors are not accumulated but only depend on the truncation error in the approximation of the velocity using the imposed displacements at the specific time considered. Therefore, the error in the amplitude of the calculated velocity in the Bathe method is $O(\Delta t^2)$, both locally and globally.

2.2.2. Acceleration results

Similarly, Eq. (24) gives the error in the acceleration at $t+\Delta t$ as

$$ {}^{t+\Delta t}\ddot{r}_p = \frac{1}{\Delta t}\left({}^{t}\dot{r}_p - 4{}^{t+\frac{\Delta t}{2}}\dot{r}_p + 3{}^{t+\Delta t}\dot{r}_p\right) + \frac{1}{\Delta t}\left(\dot{u}_p(t) - 4\dot{u}_p\left(t+\frac{\Delta t}{2}\right) + 3\dot{u}_p(t+\Delta t)\right) - \ddot{u}_p(t+\Delta t) \tag{32}$$

or

$$ {}^{t+\Delta t}\ddot{r}_p = \frac{1}{\Delta t}\left({}^{t}\dot{r}_p - 4{}^{t+\frac{\Delta t}{2}}\dot{r}_p + 3{}^{t+\Delta t}\dot{r}_p\right) + O^{l}\left(\Delta t^2\right) \tag{33}$$

Since the Bathe method uses the TR in its first sub-step, the error in velocity at $t+\frac{\Delta t}{2}$ is obtained using Eq. (15) as

$$ {}^{t+\frac{\Delta t}{2}}\dot{r}_p = -{}^{t}\dot{r}_p + O^{l}\left(\Delta t^2\right) \tag{34}$$

Substituting Eqs. (31) and (34) into Eq. (33), we have

$$ {}^{t+\Delta t}\ddot{r}_p = \frac{5}{\Delta t}{}^{t}\dot{r}_p + O^{l}(\Delta t) \tag{35}$$

Hence the error in the acceleration at $t+\Delta t$ is

$$ {}^{n\Delta t}\ddot{r}_p = \begin{cases} \frac{5}{\Delta t}{}^{0}\dot{r}_p + O^{l}(\Delta t) & \text{at the first step} \\ O^{l}(\Delta t) & \text{otherwise} \end{cases} \tag{36}$$

Note that we have an error only at the first step of order $O(\Delta t^{-1})$. However, considering the eigenvalues of $\bar{\mathbf{A}}_{\mathrm{BM}}$, the error in acceleration is not accumulated as the time integration progresses: the error at time $t+\Delta t$ is only determined by the truncation error at the time point of interest. Therefore, the acceleration error at a given time point except at $t=\Delta t$ is proportional to Δt.

An important observation is that the overshoot in the acceleration at the first step is a result of the first term on the righthand side of Eq. (33). Since ${}^{t+\Delta t}\dot{r}_p = O^{l}(\Delta t^2)$ (see Eq. (31)), we may eliminate the $O(\Delta t^{-1})$ term using the condition ${}^{t+\Delta t/2}\dot{r}_p = (1/4){}^{t}\dot{r}_p$. This condition is satisfied when using the Newmark method with $\alpha = (4/3)\delta$, but only for the first step instead of using the TR.

The analysis then shows that if we use $\alpha = (4/3)\delta$ only for the first step, and $\alpha = 1/4$ and $\delta = 1/2$ thereafter, the acceleration residual becomes

$$ {}^{n\Delta t}\ddot{r}_p = \begin{cases} \frac{5}{16}{}^{0}\ddot{r}_p + O^{l}(\Delta t) & \text{at the first step} \\ O^{l}(\Delta t) & \text{otherwise} \end{cases} \tag{37}$$

While the use of $\alpha = (4/3)\delta$ only for the first step changes the acceleration error at the first step, the velocity error is still as before, that is, ${}^{t+\Delta t}\dot{r}_p = O^{l}(\Delta t^2)$ for all time points. Note that the use of $\alpha = (4/3)\delta$ only at the first step also eliminates the acceleration overshoot at the first step when a general structure with stiff and flexible parts is solved [17].

2.3. Error propagations through the finite element model

We now consider how the errors induced at the supports where displacements are prescribed in the solution of a multiple degree of freedom system propagate to the other nodal values.

The finite element equations in Eq. (1) can be rewritten as

$$ \begin{bmatrix} \mathbf{M}_{pp} & \mathbf{M}_{pf} \\ \mathbf{M}_{fp} & \mathbf{M}_{ff} \end{bmatrix} \begin{bmatrix} \ddot{\mathbf{U}}_p \\ \ddot{\mathbf{U}}_f \end{bmatrix} + \begin{bmatrix} \mathbf{C}_{pp} & \mathbf{C}_{pf} \\ \mathbf{C}_{fp} & \mathbf{C}_{ff} \end{bmatrix} \begin{bmatrix} \dot{\mathbf{U}}_p \\ \dot{\mathbf{U}}_f \end{bmatrix} + \begin{bmatrix} \mathbf{K}_{pp} & \mathbf{K}_{pf} \\ \mathbf{K}_{fp} & \mathbf{K}_{ff} \end{bmatrix} \begin{bmatrix} \mathbf{U}_p \\ \mathbf{U}_f \end{bmatrix} = \begin{bmatrix} \mathbf{F}_p \\ \mathbf{F}_f \end{bmatrix} \tag{38}$$

where the $\mathbf{U}_p$ and $\mathbf{U}_f$ are the prescribed and from the solution "found" displacement vectors, (hence the subscripts p and f), respectively.

The solutions at time $t+\Delta t$, ${}^{t+\Delta t}\mathbf{U}_f$, ${}^{t+\Delta t}\dot{\mathbf{U}}_f$ and ${}^{t+\Delta t}\ddot{\mathbf{U}}_f$, are obtained using Eq. (38) with ${}^{t+\Delta t}\mathbf{U}_p = \mathbf{U}_p(t+\Delta t)$:

$$ \mathbf{M}_{ff}{}^{t+\Delta t}\ddot{\mathbf{U}}_f + \mathbf{C}_{ff}{}^{t+\Delta t}\dot{\mathbf{U}}_f + \mathbf{K}_{ff}{}^{t+\Delta t}\mathbf{U}_f = \bar{\mathbf{F}}_f(t+\Delta t) + {}^{t+\Delta t}\bar{\mathbf{F}}_r \tag{39}$$

where

$$\bar{\mathbf{F}}_f(t+\Delta t) = {}^{t+\Delta t}\mathbf{F}_f - \mathbf{M}_{fp}\ddot{\mathbf{U}}_p(t+\Delta t) - \mathbf{C}_{fp}\dot{\mathbf{U}}_p(t+\Delta t) - \mathbf{K}_{fp}\mathbf{U}_p(t+\Delta t) \quad (40)$$

$${}^{t+\Delta t}\bar{\mathbf{F}}_r = -\mathbf{M}_{fp}\,{}^{t+\Delta t}\ddot{\mathbf{r}}_p - \mathbf{C}_{fp}\,{}^{t+\Delta t}\dot{\mathbf{r}}_p \quad (41)$$

and ${}^{t+\Delta t}\mathbf{F}_f$ are known externally applied nodal point loads, and $\mathbf{F}_p$ could be calculated at the end of the solution.

Eqs. (39)–(41) show that the velocity and acceleration errors introduced at the prescribed degrees of freedom, ${}^{t+\Delta t}\dot{\mathbf{r}}_p$ and ${}^{t+\Delta t}\ddot{\mathbf{r}}_p$, affect the solution of the other part of the finite element model, namely through the vector, ${}^{t+\Delta t}\bar{\mathbf{F}}_r$.

2.3.1. Trapezoidal Rule

In the modal equations of Eq. (38), the TR may be expressed in the form

$$\begin{bmatrix} {}^{t+\Delta t}\ddot{x} \\ {}^{t+\Delta t}\dot{x} \\ {}^{t+\Delta t}x \end{bmatrix} = \mathbf{A}_{\mathrm{TR}} \begin{bmatrix} {}^{t}\ddot{x} \\ {}^{t}\dot{x} \\ {}^{t}x \end{bmatrix} + \mathbf{L}_{\mathrm{TR}}\left(f(t+\Delta t) + {}^{t+\Delta t}f_r\right) \quad (42)$$

where $\mathbf{A}_{\mathrm{TR}}$ and $\mathbf{L}_{\mathrm{TR}}$ are the integration approximation and load operators, respectively, x denotes a typical modal displacement, and $f(t)$ and ${}^{t}f_r$ are the modal external load and load residual, respectively, as a result of $\bar{\mathbf{F}}_f(t+\Delta t)$ and ${}^{t+\Delta t}\bar{\mathbf{F}}_r$.

The modal load residual ${}^{t}f_r$ can be expressed as

$${}^{t}f_r = c_o c_M\,{}^{t}\ddot{r}_p + c_0 c_C\,{}^{t}\dot{r}_p \quad (43)$$

where c_0, c_M and c_C are constants. The constant c_0 is determined by $\mathbf{M}_{ff}$ and $\mathbf{K}_{ff}$, and c_M and c_C are determined by $\mathbf{M}_{fp}$ and $\mathbf{C}_{fp}$. Note that c_M is zero when the lumped mass matrix is used, $\mathbf{M}_{fp}=0$, and c_C is zero when $\mathbf{C}_{fp}=0$; therefore the velocity and acceleration residuals at the prescribed displacements do not propagate to other degrees of freedom when using the lumped mass matrix and no damping matrix.

With Eqs. (39)–(43), the propagation of the errors due to the prescribed displacement is obtained in the modal equation as

$$\begin{bmatrix} {}^{t+\Delta t}\ddot{r}_f \\ {}^{t+\Delta t}\dot{r}_f \\ {}^{t+\Delta t}r_f \end{bmatrix} = \mathbf{A}_{\mathrm{TR}} \begin{bmatrix} {}^{t}\ddot{r}_f \\ {}^{t}\dot{r}_f \\ {}^{t}r_f \end{bmatrix} + \mathbf{L}_{\mathrm{TR}}\,{}^{t+\Delta t}f_r + \mathbf{O}^{I}\left(\Delta t^3\right) \quad (44)$$

where

$$\mathbf{A}_{\mathrm{TR}} = \frac{1}{\beta}\begin{bmatrix} -\omega\Delta t\,(\omega\Delta t + 4\,\xi) & -4\,\omega\,(\omega\Delta t + 2\xi) & -4\,\omega^2 \\ 2\Delta t & -\omega^2\Delta t^2 + 4 & -2\,\omega^2\Delta t \\ \Delta t^2 & 2\xi\omega\Delta t^2 + 4\Delta t & 4\,\xi\omega\Delta t + 4 \end{bmatrix};$$
$$\mathbf{L}_{\mathrm{TR}} = \frac{1}{\beta}\begin{bmatrix} 4 \\ 2\Delta t \\ \Delta t^2 \end{bmatrix};\quad \beta = \omega^2\Delta t^2 + 4\,\xi\omega\,\Delta t + 4 \quad (45)$$

Table 1
Errors in velocity and acceleration at the point of imposed displacement using the Trapezoidal Rule and the Bathe method for a linearly prescribed displacement.

	Trapezoidal Rule		Bathe method	
	${}^{t}\dot{r}_p$	${}^{t}\ddot{r}_p$	${}^{t}\dot{r}_p$	${}^{t}\ddot{r}_p$
$t=0$	$-v$	0	$-v$	0
$t=\Delta t$	v	$\frac{4v}{\Delta t}$	0	$\frac{-5v}{\Delta t}$
$t=2\Delta t$	$-v$	$-\frac{8v}{\Delta t}$	0	0
$t=3\Delta t$	v	$\frac{12v}{\Delta t}$	0	0
$\vdots$	$\vdots$			
$t=n\Delta t$	$(-1)^{n+1}v$	$\frac{(-1)^{n+1}4nv}{\Delta t}$	0	0

Substituting the expression of β and using a Taylor series expansion with respect to Δt to identify the terms on Δt we obtain

$$\mathbf{A}_{\mathrm{TR}} = \begin{bmatrix} -\xi\omega\Delta t + O(\Delta t^2) & -2\,\xi\omega + (2\xi^2\omega^2 - \omega^2)\Delta t + O(\Delta t^2) & -\omega^2 + \xi\omega^3\Delta t + O(\Delta t^2) \\ \frac{1}{2}\Delta t + O(\Delta t^2) & 1 - \xi\omega\Delta t + O(\Delta t^2) & -\frac{\omega^2}{2}\Delta t + O(\Delta t^2) \\ \frac{1}{4}\Delta t^2 & \Delta t - \frac{1}{2}\xi\omega\Delta t^2 & 1 - \frac{1}{4}\omega^2\Delta t^2 \end{bmatrix} + \mathbf{O}^{I}(\Delta t^3) \quad (46)$$

$$\mathbf{L}_{\mathrm{TR}} = \begin{bmatrix} 1 - \xi\omega\Delta t + O(\Delta t^2) \\ \frac{1}{2}\Delta t - \frac{1}{2}\xi\omega\Delta t^2 \\ \frac{1}{4}\Delta t^2 \end{bmatrix} + \mathbf{O}(\Delta t^3) \quad (47)$$

Focusing on ${}^{t}\ddot{r}_f, {}^{t}\dot{r}_f$ and ${}^{t}r_f$ in Eq. (44), we may identify some convergence behaviors of these quantities.

If we consider the case of a consistent mass matrix, ${}^{t}f_r$ is proportional to ${}^{t}\ddot{r}_p$ whose magnitude is proportional to Δt^{-1} locally, and Δt^{-2} globally (see, Eqs. (21) and (43)). As the leading term in $\mathbf{L}_{\mathrm{TR}}(1)$ is $O^{I}(0)$, the magnitude of the acceleration error ${}^{t}\ddot{r}_f$ is also proportional to Δt^{-1} locally, and Δt^{-2} globally. Also, considering the terms in $\mathbf{A}_{\mathrm{TR}}$ and $\mathbf{L}_{\mathrm{TR}}$, we observe that the order of error in velocity is limited to $O(0)$ globally. We will illustrate the step-by-step error propagations with a simple example in Section 2.4.

2.3.2. Bathe method

Similarly, the Bathe method is expressed in the modal equation of Eq. (39) as

$$\begin{bmatrix} {}^{t+\Delta t}\ddot{x} \\ {}^{t+\Delta t}\dot{x} \\ {}^{t+\Delta t}x \end{bmatrix} = \mathbf{A}_{\mathrm{BM}} \begin{bmatrix} {}^{t}\ddot{x} \\ {}^{t}\dot{x} \\ {}^{t}x \end{bmatrix} + \mathbf{L}_{\mathrm{a}}\left(f(t+\Delta t/2) + {}^{t+\Delta t/2}f_r\right) + \mathbf{L}_{\mathrm{b}}\left(f(t+\Delta t) + {}^{t+\Delta t}f_r\right) \quad (48)$$

where $\mathbf{A}_{\mathrm{BM}}$ is the integration approximation operator, and $\mathbf{L}_{\mathrm{a}}$ and $\mathbf{L}_{\mathrm{b}}$ are the load operators.

With Eq. (48), the recursive form of the errors is

$$\begin{bmatrix} {}^{t+\Delta t}\ddot{r}_f \\ {}^{t+\Delta t}\dot{r}_f \\ {}^{t+\Delta t}r_f \end{bmatrix} = \mathbf{A}_{\mathrm{BM}} \begin{bmatrix} {}^{t}\ddot{r}_f \\ {}^{t}\dot{r}_f \\ {}^{t}r_f \end{bmatrix} + \mathbf{L}_{\mathrm{a}}\, {}^{t+\Delta t/2}f + \mathbf{L}_{\mathrm{b}}\, {}^{t+\Delta t}f_r + \mathbf{O}^{l}\left(\Delta t^3\right) \tag{49}$$

where with the use of the Taylor series expansion

$$\mathbf{A}_{\mathrm{BM}} = \begin{bmatrix} -\frac{2\xi\omega}{3}\Delta t + O\left(\Delta t^2\right) & -2\,\xi\omega + \left(\frac{8}{3}\xi^2\omega^2 - \omega^2\right)\Delta t + O\left(\Delta t^2\right) & -\omega^2 + \frac{4}{3}\xi\omega^3\Delta t + O\left(\Delta t^2\right) \\ \frac{1}{3}\Delta t + O\left(\Delta t^2\right) & 1 - \frac{4}{3}\xi\omega\Delta t + O\left(\Delta t^2\right) & -\frac{2\omega^2}{3}\Delta t + O\left(\Delta t^2\right) \\ \frac{7}{36}\Delta t^2 & \Delta t - \frac{11}{18}\xi\omega\Delta t^2 & 1 - \frac{11}{36}\omega^2\Delta t^2 \end{bmatrix} + \mathbf{O}\left(\Delta t^3\right)$$

$$\mathbf{L}_{\mathrm{a}} = \begin{bmatrix} -\frac{2\xi\omega}{3}\Delta t + O\left(\Delta t^2\right) \\ \frac{1}{3}\Delta t + O\left(\Delta t^2\right) \\ \frac{7}{36}\Delta t^2 \end{bmatrix} + \mathbf{O}\left(\Delta t^3\right), \qquad \mathbf{L}_{\mathrm{b}} = \begin{bmatrix} 1 - \frac{2}{3}\xi\omega\Delta t + O\left(\Delta t^2\right) \\ \frac{1}{3}\Delta t + O\left(\Delta t^2\right) \\ \frac{1}{9}\Delta t^2 \end{bmatrix} + \mathbf{O}\left(\Delta t^3\right) \tag{50}$$

Considering the case of a consistent mass matrix, ${}^{t}f_r$ is proportional to ${}^{t}\ddot{r}_p$ which is $O(\Delta t)$. Due to the leading term in $\mathbf{L}_{\mathrm{b}}(1)$, the error in ${}^{t}\ddot{r}_f$ due to ${}^{t}\ddot{r}_p$ is also $O(\Delta t)$. Furthermore, the leading terms in $\mathbf{A}_{\mathrm{BM}}$ show that the order of ${}^{t}\ddot{r}_f$, ${}^{t}\dot{r}_f$ and ${}^{t}r_f$ is limited to $O(0)$, globally.

2.4. Example solution: Imposed displacement of constant velocity

To obtain insight we consider the simple 1-degree of freedom case in which the displacement is prescribed linearly

$${}^{t}u_p = u_p(t) = vt \tag{51}$$

Hence the exact solution is $\dot{u}_p(t) = v$, $\ddot{u}_p(t) = 0$. However, we use the initial conditions ${}^{0}\dot{u}_p = 0$ and ${}^{0}\ddot{u}_p = 0$ for the time integration. Hence, we see that an error is introduced for the velocity at time zero.

Clearly

$${}^{0}\dot{r}_p = -v;\ {}^{0}\ddot{r}_p = 0 \tag{52}$$

Table 2
Errors in displacement, velocity and acceleration for free degrees of freedom using the Trapezoidal Rule and the Bathe method; for a linearly prescribed displacement with consistent mass matrix and zero damping; $O(\Delta t^2)$ and higher-order terms are omitted.

	Trapezoidal Rule			Bathe method		
	r_f	$\dot{r}_f$	$\ddot{r}_f$	r_f	$\dot{r}_f$	$\ddot{r}_f$
$t=0$	0	0	a_0	0	0	a_0
$t=\Delta t$	$v\Delta t$	$2v$	$\frac{4v}{\Delta t}$	$v\Delta t$	v	$-\frac{5v}{\Delta t}$
$t=2\Delta t$	$2v\Delta t$	0	$-\frac{8v}{\Delta t}$	$2v\Delta t$	v	$-2v\Delta t$
$t=3\Delta t$	$3v\Delta t$	$2v$	$\frac{12v}{\Delta t}$	$3\ v\Delta t$	v	$-3v\Delta t$
$\vdots$	$\vdots$					
$t=n\Delta t$	$nv\Delta t$	$(1+(-1)^{n+1})v$	$(-1)^{n+1}\frac{4nv}{\Delta t}$	$nv\Delta t$	v	$-nv\Delta t$

For the TR, for all t, as ${}^{t+\Delta t}u_p = v(t+\Delta t)$, ${}^{t}u_p = vt$ and $\dot{u}_p(t) = \dot{u}_p(t+\Delta t) = v$, we have

$$\frac{2}{\Delta t}\left({}^{t+\Delta t}u_p - {}^{t}u_p\right) - \dot{u}_p(t) - \dot{u}_p(t+\Delta t) = 0 \tag{53}$$

Similarly, also with $\ddot{u}_p(t) = \ddot{u}_p(t+\Delta t) = 0$, we have

$$\frac{4}{\Delta t^2}\left({}^{t+\Delta t}u_p - {}^{t}u_p\right) - \frac{4}{\Delta t}\dot{u}_p(t) - \ddot{u}_p(t+\Delta t) - \ddot{u}_p(t) = 0 \tag{54}$$

Substituting Eqs. (53) and (54) into Eqs. (13) and (19), respectively, we obtain

$$\begin{aligned} {}^{t+\Delta t}\dot{r}_p &= -{}^{t}\dot{r}_p \\ {}^{t+\Delta t}\ddot{r}_p &= -\frac{4}{\Delta t}{}^{t}\dot{r}_p - {}^{t}\ddot{r}_p \end{aligned} \tag{55}$$

Therefore

$$\begin{aligned} {}^{n\Delta t}\dot{r}_p &= (-1)^{n+1}v \\ {}^{n\Delta t}\ddot{r}_p &= (-1)^{n+1}\frac{4nv}{\Delta t} \end{aligned} \tag{56}$$

Of course, this result corresponds to the use of the matrix $\bar{\mathbf{A}}_{\mathrm{TR}}$ applied to the propagation of the error through time. The results for the first few time steps are given in Table 1.

The table shows that the error in the velocity has a high frequency oscillation of period $2\Delta t$ and amplitude v, whereas the error in the acceleration has a high frequency oscillation of period $2\Delta t$ and rapidly growing amplitude. The amplitude at time $t = n\Delta t$ is

$$\left|{}^{n\Delta t}\ddot{r}_p\right| = \frac{4nv}{\Delta t} = \frac{4n\Delta t v}{\Delta t^2} = \frac{4vt}{\Delta t^2} \tag{57}$$

As expected in Section 2.1.2, for a given time t, the error in the amplitude becomes worse as we decrease the time step size, in fact the amplitude error is proportional to Δt^{-2}.

Considering next the Bathe method, Eqs. (30) and (32) give

$${}^{n\Delta t}\dot{r}_p = 0 \tag{58}$$

$${}^{n\Delta t}\ddot{r}_p = \begin{cases} \frac{-5}{\Delta t}v & \text{at the first step} \\ 0 & \text{otherwise} \end{cases} \tag{59}$$

Important observations are that, unlike when using the TR, the velocity error is set zero already in the first step, and the velocity error at $t = 0$ only affects the acceleration results in the first step with no propagation to the time points thereafter. The errors at any point in time using

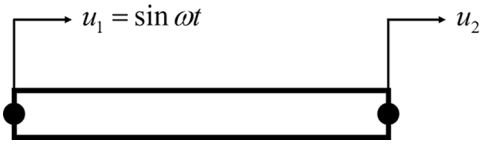

Fig. 1. A 2-node finite element under sinusoidal prescribed displacement; $\omega = 1.2$; with initial conditions ${}^0u_2 = {}^0\dot{u}_1 = {}^0\dot{u}_2 = {}^0\ddot{u}_1 = {}^0\ddot{u}_2 = 0$.

the Bathe method only depend on the truncation error of the imposed displacements. Therefore, in the Bathe method, the error at time $t = n\Delta t$ is zero except for the acceleration in the first step.

We can now assess the errors seen in all degrees of freedom in the solution of multiple degree of freedom finite element models when only some nodal displacements are imposed.

As ${}^t\dot{r}_p$ and ${}^t\ddot{r}_p$ are now given, ${}^tf_r$ is known for all time points; therefore, we may calculate, in a step-by-step manner, the errors in a typical modal solution corresponding to the free degrees of freedom with the recursive relation in Eqs. (44) and (49) for the TR and the Bathe method, respectively.

Table 2 shows the results of first few time steps for the case of a consistent mass matrix and zero damping. As pointed out in Sections 2.3.1 and 2.3.2, in both the Trapezoidal Rule and the Bathe method, ${}^t\ddot{r}_p$ is directly transferred to ${}^t\ddot{r}_f$ due to the $O(0)$ term in the load operator.

Using the TR, the amplitude of ${}^{n\Delta t}\ddot{r}_f$ is proportional Δt^{-2}, as is ${}^{n\Delta t}\ddot{r}_p$, while the errors in displacement and velocity are independent of the time step size. Here note that the amplitude of r_f at time $t = n\Delta t$ is independent of the time step size since ${}^{n\Delta t}r_f = nv\Delta t = vt$.

Using the Bathe method, on the other hand, as ${}^t\ddot{r}_p$ is zero except for the first step, the errors are solely determined by $\mathbf{A}_{\mathrm{BM}}$ and we see that the magnitudes of all errors are independent of the time step size.

3. Illustrative numerical solutions

We consider a simple problem of one 2-node (truss) finite element and a two-dimensional wave propagation problem to illustrate the errors induced by imposed displacements. The 2-node element solution (in

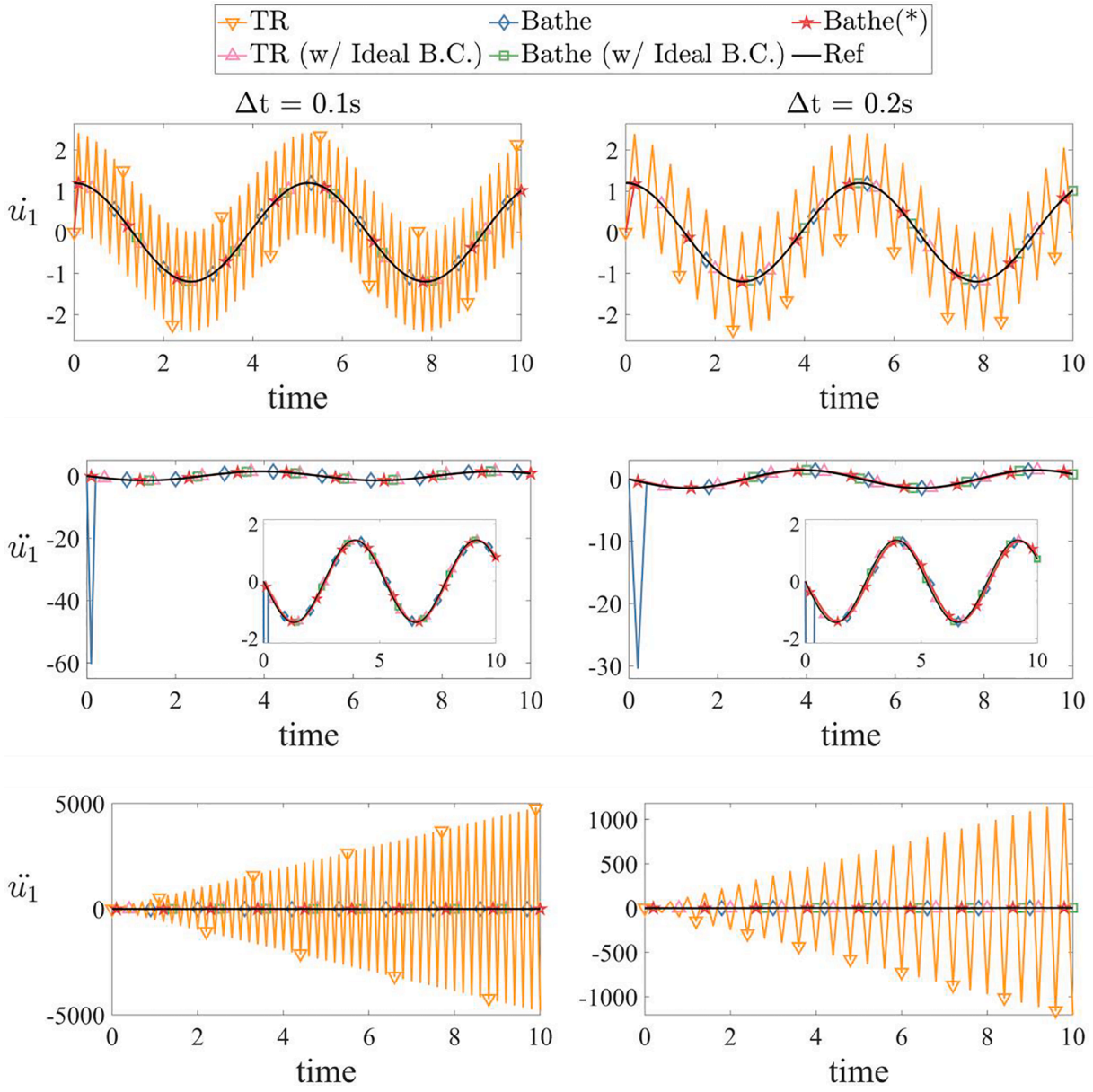

Fig. 2. Predictions of velocity and acceleration at node 1; "Bathe(*)" uses $\alpha = 1$ and $\delta = 3/4$ only for the first step, and $\alpha = 1/4$ and $\delta = 1/2$ otherwise; the results of the computed acceleration for "TR" are shown separately due to the different scale.

Section 3.1) is proposed as an appropriate problem to solve in the *patch test* for time integration schemes mentioned earlier.

3.1. A linear finite element under sinusoidal prescribed displacement

We consider the simple two degree-of-freedom problem shown in Fig. 1 with the imposed displacement, $u_1(t) = \sin(1.2t)$ and demonstrate the response obtained. For the model we consider the cases of consistent and lumped mass matrices, $\mathbf{M}_C$ and $\mathbf{M}_L$, respectively, with a zero or non-zero damping matrix, $\mathbf{C}$:

$$\mathbf{M}_C = \frac{1}{6}\begin{bmatrix} 2 & 1 \\ 1 & 2 \end{bmatrix}; \mathbf{M}_L = \frac{1}{2}\begin{bmatrix} 1 & 0 \\ 0 & 1 \end{bmatrix}; \mathbf{K} = \begin{bmatrix} 1 & -1 \\ -1 & 1 \end{bmatrix}; \mathbf{C} = 0.1\mathbf{M} + 0.2\mathbf{K} \tag{60}$$

where $\mathbf{K}$ is the stiffness matrix. We propose that this model be solved as part of the patch test discussed in Section 1 (to test for the fourth property).

Since the imposed displacement has an analytical form, $u_1(t) = \sin(1.2t)$, the exact expressions for the corresponding imposed velocity and acceleration are available. However, in practice, mostly only the values for imposed displacements are available, and the corresponding velocities and accelerations are calculated numerically in the time integration. Hence we use the *exact* imposed displacement and the *calculated* velocity and acceleration for node 1 as the primary case to focus on. In this procedure, we use Eqs. (7) and (28) for the TR and the Bathe method, respectively, and we refer to this case as the "usual B.C." case.

Yet, to also illustrate the effect of the errors due to the calculated imposed velocity and acceleration, we also use the exact values of velocitiy and acceleration, $\dot{u}_1(t) = 1.2\cos(1.2t)$ and $\ddot{u}_1(t) = -1.44\sin(1.2t)$. We refer to the results with these analytical boundary conditions for displacement, velocity and acceleration as the "ideal B.C." case.

Figs. 2–4 give the results of the case when the mass matrix $\mathbf{M}_C$ and the non-zero matrix $\mathbf{C}$ are considered. We show the results using the Trapezoidal Rule and the Bathe method with two time step sizes, Δt=0.1 and 0.2. In addition we use the Bathe method with $\alpha = 1$ and $\delta = 3/4$ only for the first step, and $\alpha = 1/4$ and $\delta = 1/2$ thereafter, and the corresponding results are referred as "Bathe (*)." The analytical solution is used as the reference.

For all solution variables, both methods for the case ideal B.C. and the Bathe method with the usual condition of only the displacement imposed (the usual B.C.) provide accurate solutions for all considered time step sizes. As expected, when using the Bathe method, there is only for the first time step an overshoot in the accelerations and reactions, see Section 2.3.2, and these overshoots are eliminated by using the parameters $\alpha = 1$ and $\delta = 3/4$ only for the first step.

Also, as theoretically established in the previous sections, when using the usual B.C. the instability in $\ddot{u}_1$ and $\ddot{u}_2$ using the TR is apparent and increases as we reduce the time step size: we observe four times larger residuals in accelerations when the time step size is halved (see Sections 2.1.2 and 2.3.1). The TR also gives constant but noticeable errors in velocities.

To see the convergence behavior of the solutions, we use the error norms

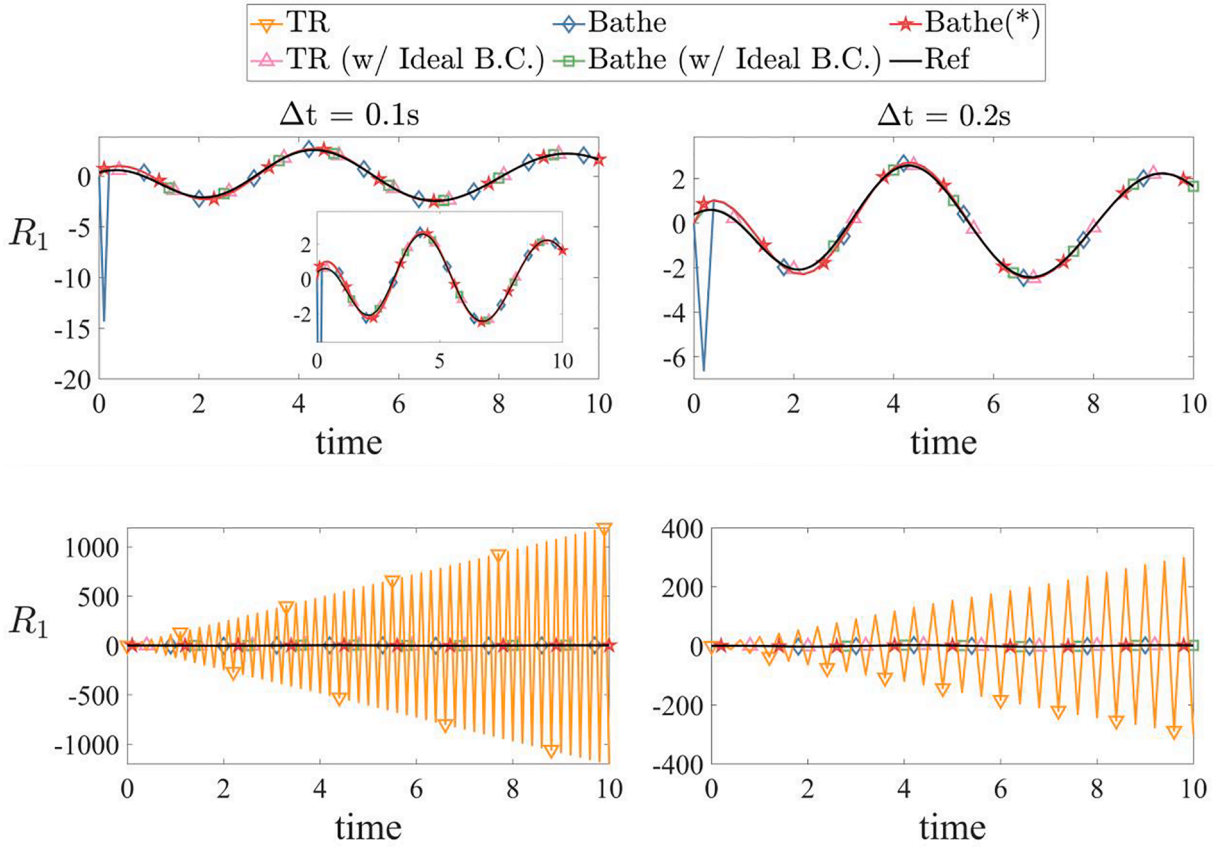

Fig. 3. Prediction of reaction force; "Bathe(*)" uses $\alpha = 1$ and $\delta = 3/4$ only for the first step, and $\alpha = 1/4$ and $\delta = 1/2$ otherwise; the results of the computed reaction for "TR" are shown separately due to the different scale.

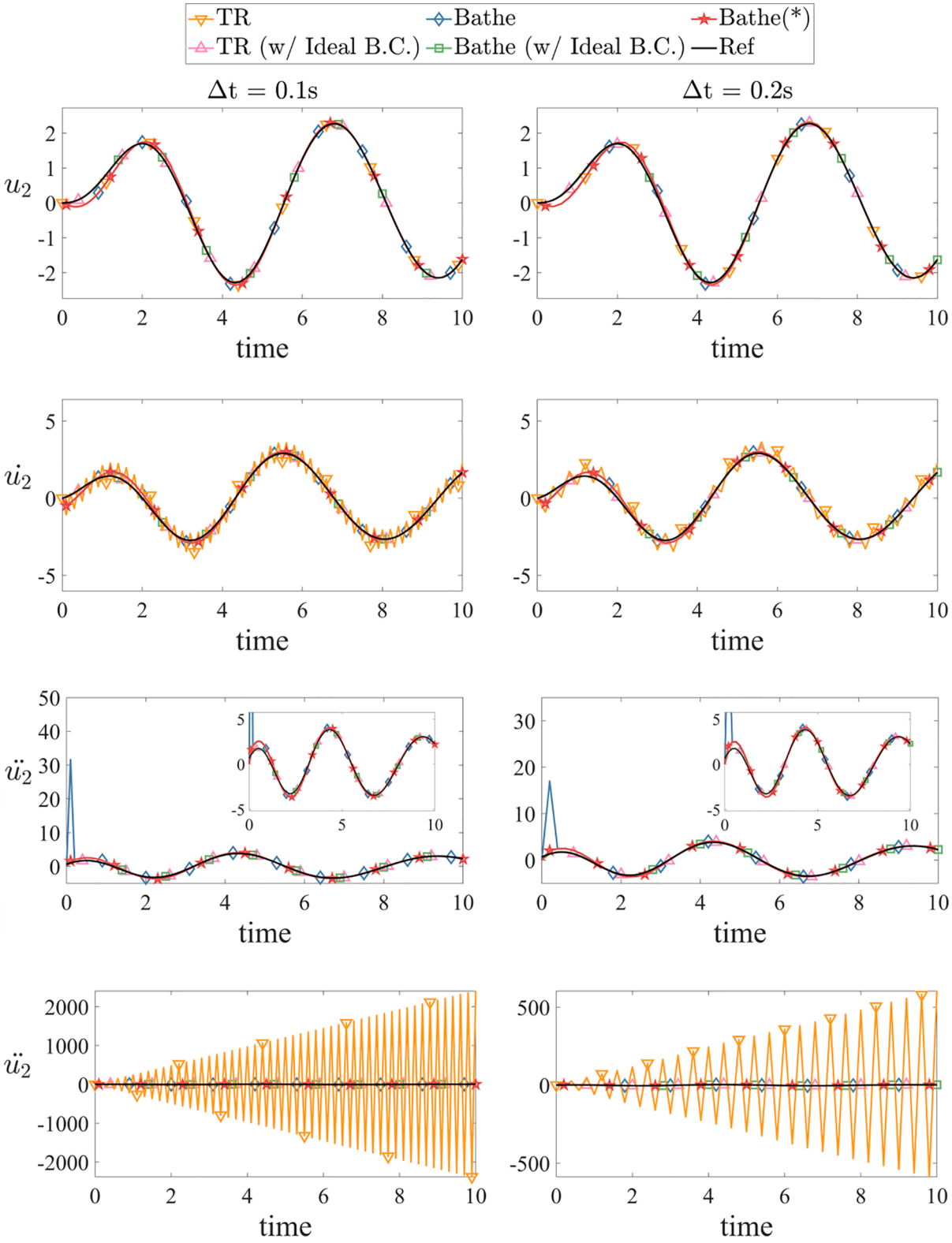

Fig. 4. Predictions of displacement, velocity and acceleration at node 2; "Bathe(*)" uses $\alpha = 1$ and $\delta = 3/4$ only for the first step, and $\alpha = 1/4$ and $\delta = 1/2$ otherwise; the results of the computed acceleration for "TR" are shown separately due to the different scale.

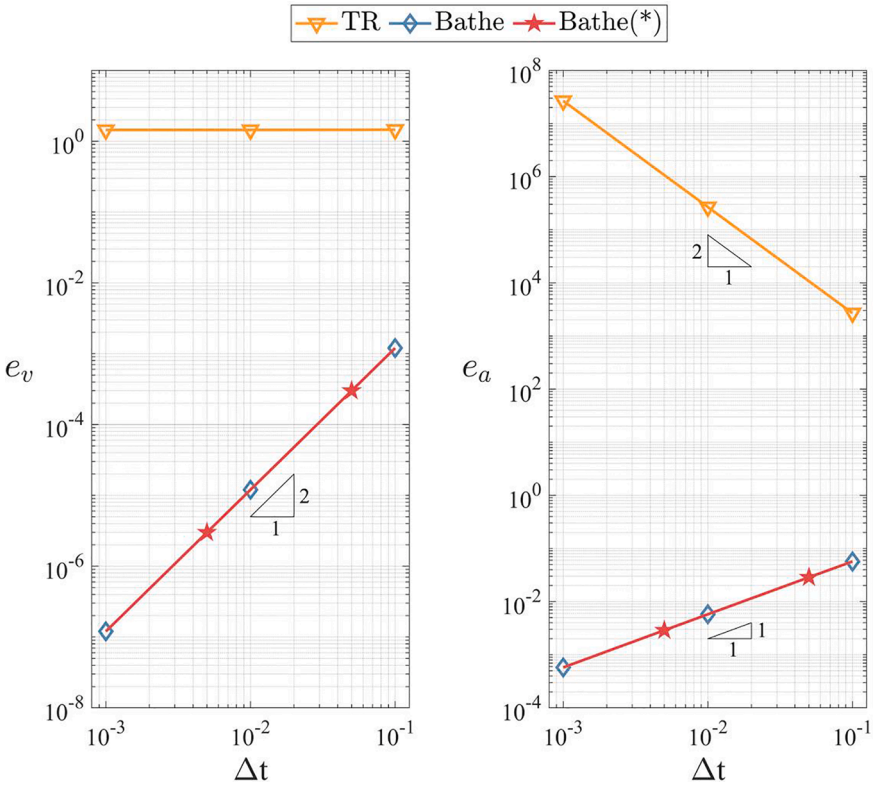

Fig. 5. Velocity and acceleration error norms at node 1, where the displacement is imposed; "Bathe(*)" uses $\alpha = 1$ and $\delta = 3/4$ only for the first step, and $\alpha = 1/4$ and $\delta = 1/2$ otherwise.

$$e_u = \left(\frac{\sum_{i=2}^{10/\Delta t} \left({}^{i\Delta t}u - u(i\Delta t) \right)^2}{\sum_{i=2}^{10/\Delta t} \left(u(i\Delta t) \right)^2} \right)^{0.5} ; \; e_v = \left(\frac{\sum_{i=2}^{10/\Delta t} \left({}^{i\Delta t}\dot{u} - \dot{u}(i\Delta t) \right)^2}{\sum_{i=2}^{10/\Delta t} \left(\dot{u}(i\Delta t) \right)^2} \right)^{0.5} ; \quad e_a = \left(\frac{\sum_{i=2}^{10/\Delta t} \left({}^{i\Delta t}\ddot{u} - \ddot{u}(i\Delta t) \right)^2}{\sum_{i=2}^{10/\Delta t} \left(\ddot{u}(i\Delta t) \right)^2} \right)^{0.5} \tag{61}$$

and focus only on the case of usual B.C.

Fig. 5 shows the error norms of the velocity and acceleration for node 1 and we see the expected order of accuracy (discussed in Section 2) for the TR and the Bathe method.

We also show the error norms of the solution variables for node 2 for various system matrices, see Fig. 6. As seen in Eq. (43), the convergence behavior may change for the type of mass matrix and the presence of physical damping. For the Bathe method with any type of system matrices, the errors in all solution variables do not increase as the time step size decreases and remain sufficiently small for both time step sizes. The different parameter set used to eliminate the first step overshoot does not provide any enhancements for overall solution accuracy. Note that for the cases of $\mathbf{M}_C$, the TR provides an *increased error* in acceleration for a *decreased time step size*, and constant but relatively large errors in velocity for both time step sizes.

3.2. A two-dimensional scalar wave propagation induced by an imposed displacement

We next consider the solution of wave propagations in the pre-stressed membrane shown in Fig. 7 for which the transverse displacement u is governed by

$$\frac{1}{c_0^2}\frac{\partial^2 u}{\partial t^2} = \frac{\partial^2 u}{\partial x^2} + \frac{\partial^2 u}{\partial y^2} \tag{62}$$

Here c_0 is the exact wave speed and we use $c_0 = 1$. We focus on solving for the wave induced by an imposed displacement at the mid-point (while we imposed an external load in previous studies [25–29]). The imposed displacement at the origin is given as

$$u(0,0,t) = 10\left(1 - 2\pi^2 f^2 t^2\right)\exp\left(-\pi^2 f^2 t^2\right) \tag{63}$$

where $f = 6$. Due to symmetry, only the domain $[0, 1] \times [0, 1]$ is discretized using four-node finite elements.

The Bathe method and the Trapezoidal Rule are used with the time step sizes determined by the CFL numbers, 1 and 0.65, respectively, to have their optimal performances [27,28]. For the CFL number $= c_0 \Delta t / x_e$, the side length of the elements is used as the characteristic length x_e.

As in Section 3.1, we consider the usual B.C., that is, we impose the exact displacement, Eq. (63), while the imposed velocity and acceleration are calculated by the time integration. For comparisons, we also

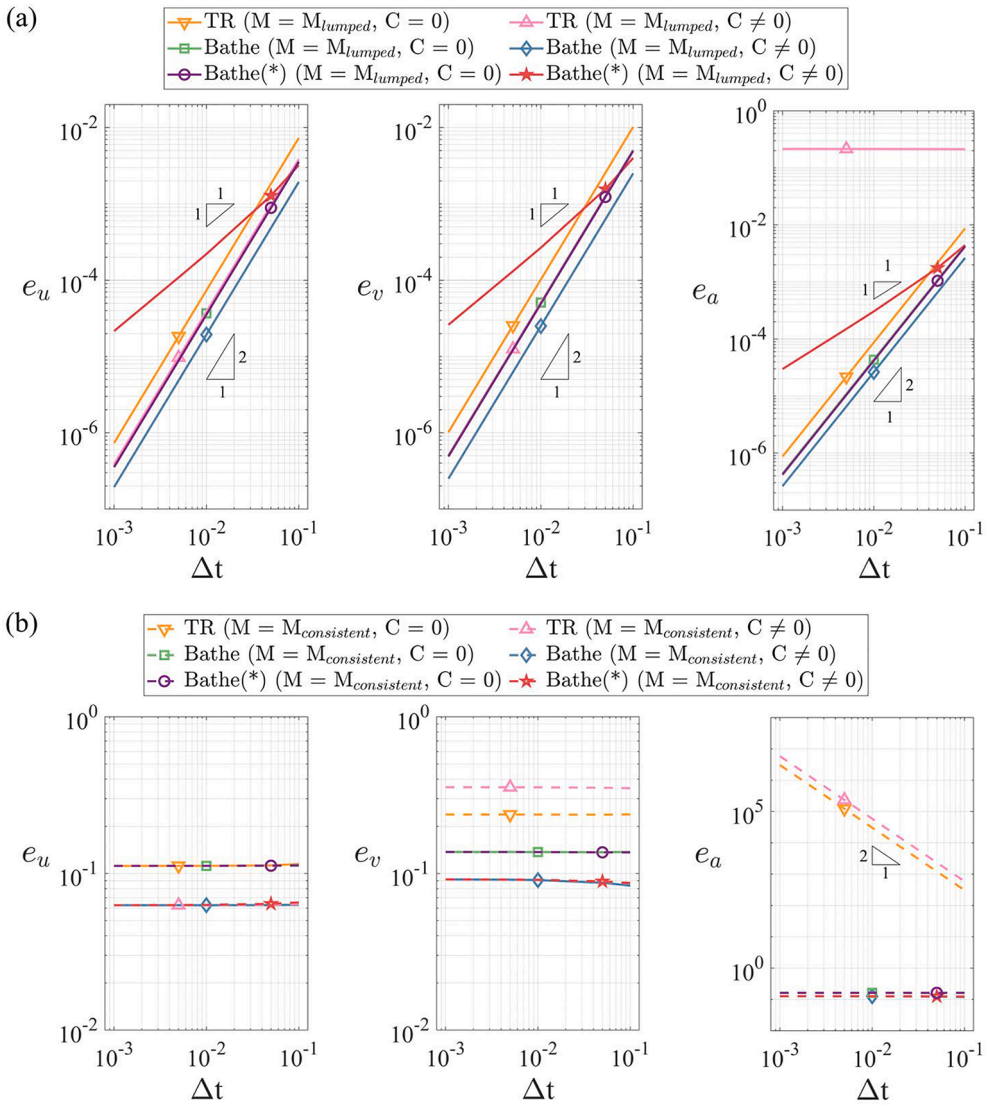

Fig. 6. Displacement, velocity and acceleration error norms at node 2 for various system matrices, (a) Lumped mass matrix and (b) Consistent mass matrix; "Bathe (*)" uses $\alpha = 1$ and $\delta = 3/4$ only for the first step, and $\alpha = 1/4$ and $\delta = 1/2$ otherwise.

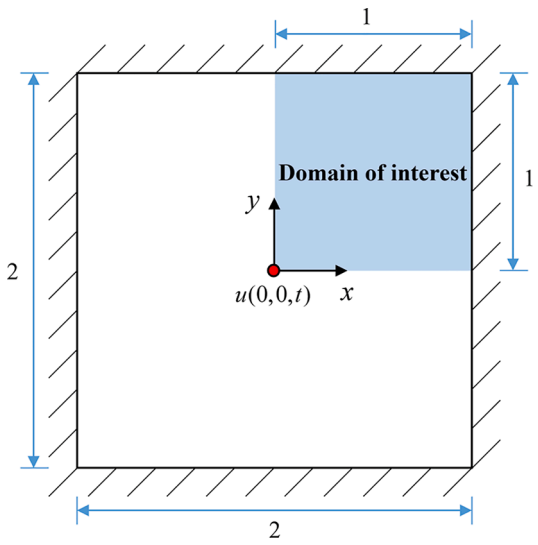

Fig. 7. 2D scalar wave problem for a pre-stressed membrane; the domain of interest is shaded.

consider ideal B.C., where we impose the exact displacement together with the exact velocity and acceleration obtained by taking derivatives on Eq. (63).

In wave propagation problems, the solution accuracy of a time integration scheme is largely determined by the numerical dispersion and it is of interest to see the effect on the dispersion when using the ideal and the usual B.C. For detailed discussions on the dispersion properties of the TR and the Bathe method see Refs. [27,28].

Figs. 8–10 show the displacement, velocity and acceleration along the x-axis using 100 × 100 and 200 × 200 element meshes. With the ideal B.C. the TR gives spurious oscillations in the velocity and acceleration due to dispersion errors, but an important observation is that the solutions with the usual B.C. show significantly larger errors. Also, the solutions become worse as we refine the mesh. In particular, the scheme provides in essence unstable solutions for the acceleration.

On the other hand, the Bathe method provides accurate solutions for both types of boundary conditions. Note that using the Bathe method, the differences in the solutions using the ideal B.C. and the usual B.C. are very small. Also, as expected, the accuracy of the solutions is increased as we increase the spatial resolution (and use correspondingly the smaller optimal time step size).

We can also see the effect of using the different prescribed displacement conditions when considering snapshots. Figs. 11 and 12 show snapshots of the solutions using the Trapezoidal Rule and the Bathe method at $t = 0.9$s. The results show that using the Bathe method, the solution difference solving with the usual or ideal B.C. is small. However, using the TR the errors due to imposing the usual B.C. severely deteriorate the solution accuracy in the whole model.

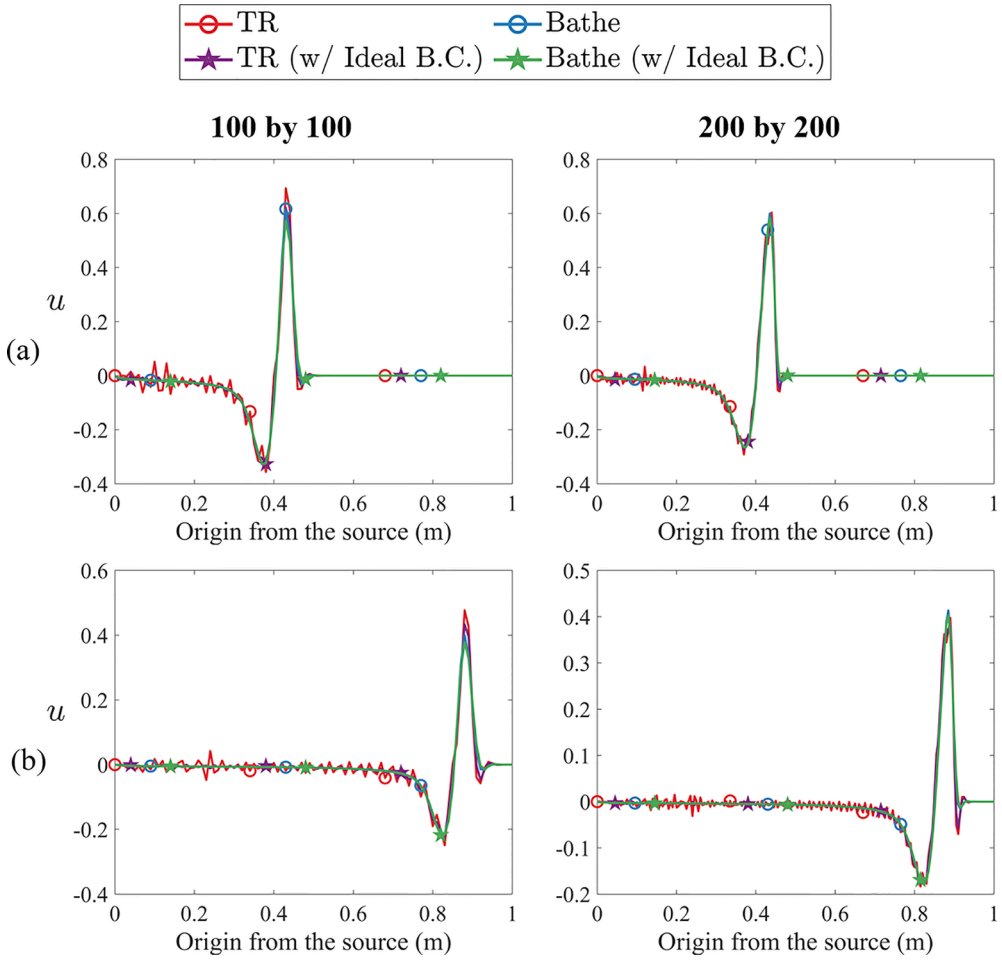

Fig. 8. Transverse displacements along the x-axis; first column: 100 by 100 element mesh; second column: 200 by 200 element mesh; (a) at $t = 0.45$ s; (b) at $t = 0.9$ s.

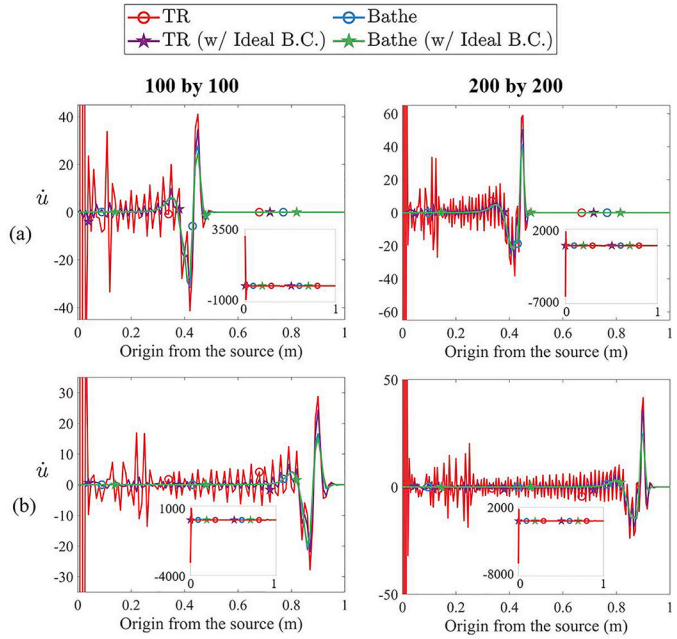

Fig. 9. Transverse velocities along the x-axis; first column: 100 by 100 element mesh; second column: 200 by 200 element mesh; (a) at $t = 0.45$ s; (b) at $t = 0.9$ s.

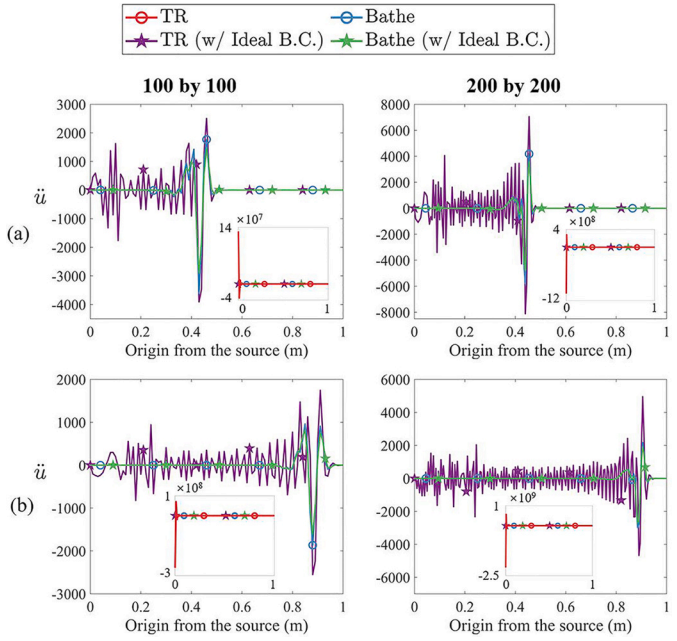

Fig. 10. Transverse accelerations along the x-axis; first column: 100 by 100 element mesh; second column: 200 by 200 element mesh; (a) at $t = 0.45$ s; (b) at $t = 0.9$ s. The result of "Trapezoidal" is only plotted in sub-figures due to the different scale.

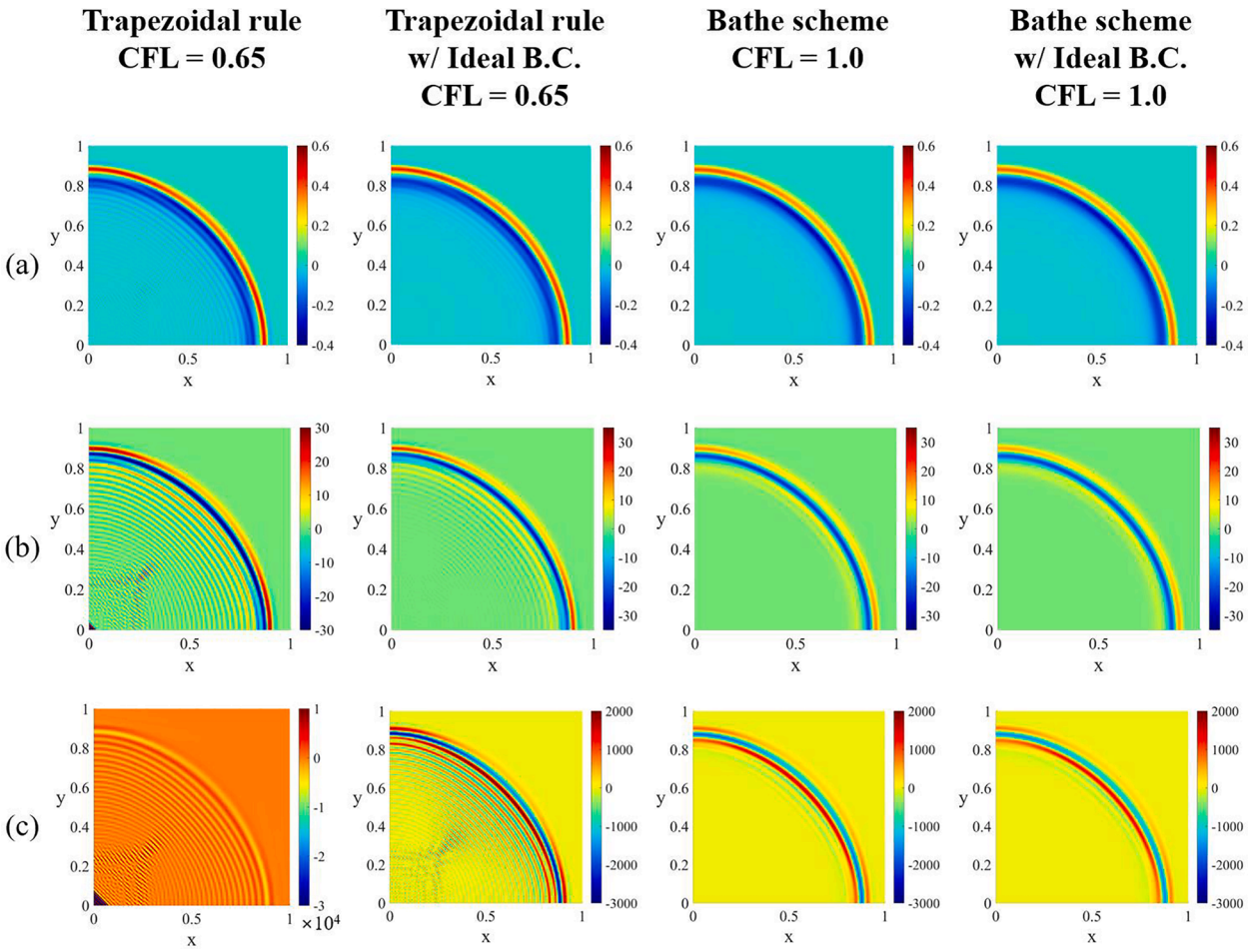

Fig. 11. Snapshots at time $t = 0.9$ s with 100 by 100 finite element mesh: (a) displacements, (b) velocities, and (c) accelerations.

4. Concluding remarks

Commonly, in the analysis of a time integration scheme, the research focuses on the stability and accuracy of a scheme when external forces or non-zero initial conditions are applied. However, there are important additional considerations when in direct time integration a structure is considered with imposed displacements. Our objective in this paper was to focus on that case because we had observed some surprising phenomena when in implicit direct time integration displacements are prescribed.

In the paper we theoretically analyzed the response of structural systems with imposed displacements when two implicit time integration schemes are used: the Trapezoidal Rule and the Bathe method. An important theoretical observation is that when using the TR quite inaccurate solutions can be obtained and the *solution errors increase* as we *decrease the time step size.* This observation is contrary to what we see in the solution of structural systems with imposed forces or nonzero initial conditions, where using the TR the solution errors decrease as we decrease the time step size.

We also found theoretically that the behavior of the solution errors is different when different system matrices are used, that is, whether a lumped mass matrix or a consistent mass matrix is used, and whether a damping matrix is included.

On the other hand, when using the Bathe method, the solution errors are reasonable and behave as an analyst would expect: *smaller errors are obtained for a smaller time step size used* – and this good behavior is seen for any system matrices used.

We illustrated all theoretical findings in two example solutions: the analysis of a simple two degree of freedom structural model and the solution of a two-dimensional wave propagation problem. These solutions displayed all our theoretical observations.

A more general thought exposed in the paper is that implicit direct time integration schemes should be analyzed using a "patch test for time integration schemes". This patch test comprises the stability and accuracy analysis for imposed forces and initial conditions and *also* the analysis of the errors on the solution variables when displacements are prescribed for any reasonable system matrices used. A simple problem with an imposed displacement for this patch test is given in Section 3.1. The patch test is passed if the method is always unconditionally stable for imposed forces, initial conditions and displacements, does not show any overshoot, and contains appropriate numerical damping. If the patch test is passed, the most effective method is the one which for a given solution accuracy requires the least amount of solution effort.

Based on the above thoughts and requirements, we have shown in this paper that the Trapezoidal Rule does not pass the patch test, and that the Bathe method passes the test. It would be valuable to perform the studies we have given in this paper also for other and recently developed schemes (e.g., [30–39]), and indeed also for novel finite

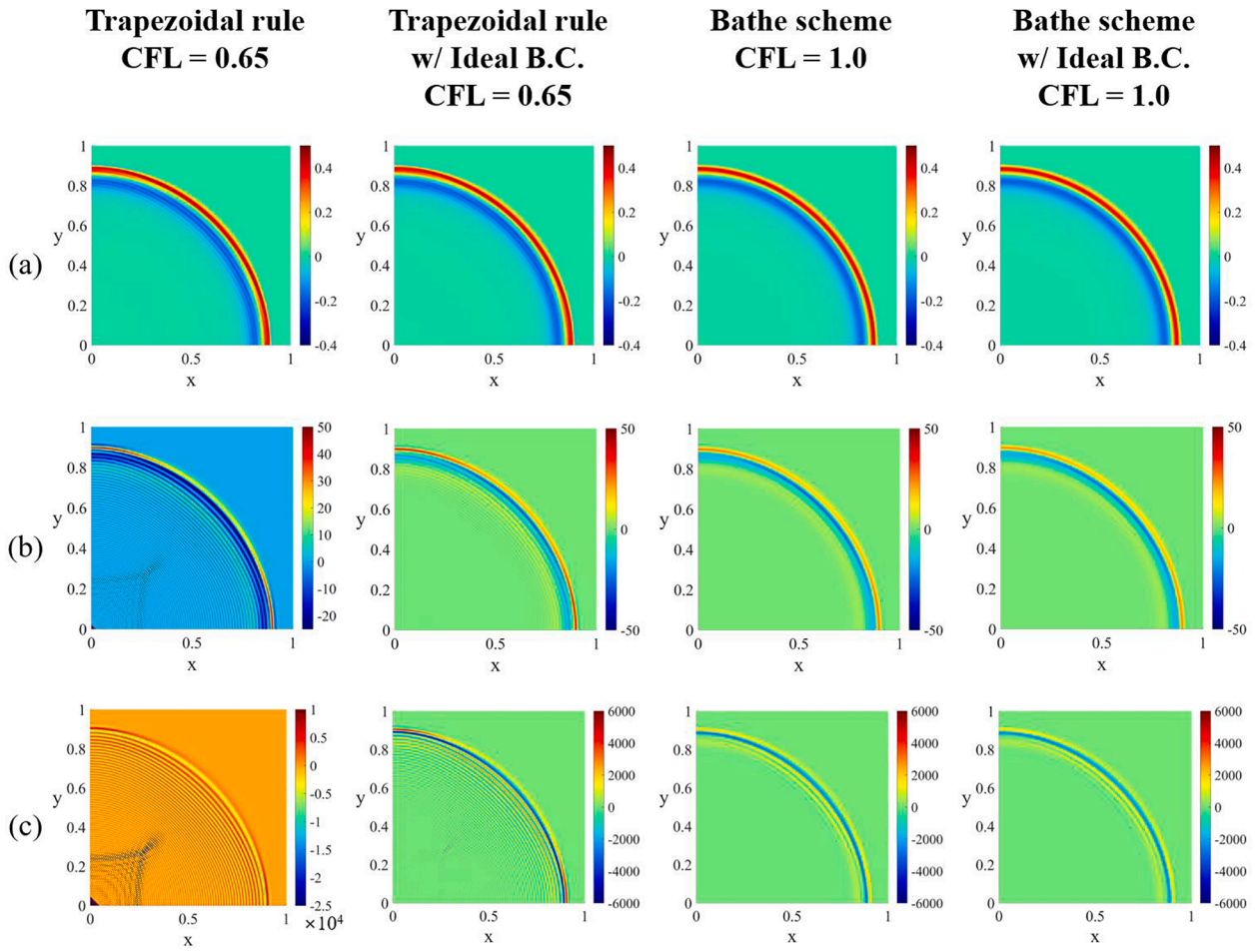

Fig. 12. Snapshots at time $t = 0.9$ s with 200 by 200 finite element mesh: (a) displacements, (b) velocities, and (c) accelerations.

element discretizations used in time integrations, like the overlapping finite elements [40].

CRediT authorship contribution statement

Gunwoo Noh: Methodology, Formal analysis, Investigation. **Klaus-Jürgen Bathe:** Conceptualization, Investigation.

Declaration of Competing Interest

The authors declare that they have no known competing financial interests or personal relationships that could have appeared to influence the work reported in this paper.

Acknowledgments

The authors would like to thank Dr. T. Sussman and Dr. J. Walczak of Bentley Systems, Inc. who identified the time integration problem considered in this paper with Dr. Sussman providing first insight to ensure that there is no coding error in ADINA. This work was partly supported by the Young Scientist Grants-Outstanding Track (Grant No. NRF-2021R1C1C1011494) through the National Research Foundation of Korea (NRF) funded by the Ministry of Science and ICT.

References

[1] Bathe KJ. The finite element method. In: Linderberg T, Wah B, editors. Encyclopedia of computer science and engineering. Hoboken, New Jersey, J: Wiley and Sons; 2009. p. 1253–64.
[2] Bathe KJ. Frontiers in finite element procedures & applications, chapter 1. In: Topping BHV, Iványi P, editors. Computational methods for engineering technology. Stirlingshire, Scotland: Saxe-Coburg Publications; 2014.
[3] Bathe KJ. Finite element procedures. Prentice Hall; 1996. 2nd ed. KJ Bathe, Watertown, MA, 2014, and Higher Education Press, Beijing, 2016.
[4] Newmark NM. A method of computation for structural dynamics. J Eng Mech Divsion 1959;85(3):67–94.
[5] Park KC. An improved stiffly stable method for direct integration of nonlinear structural dynamics. J Appl Mech Trans ASME 1975;42(2):464–70.
[6] Hilber HM, Hughes TJR, Taylor RL. Improved numerical dissipation for time integration algorithms in structural dynamics. Earthq Eng Struct Dyn 1977;5:283–92.
[7] Wood WL, Bossak M, Zienkiewicz OC. An alpha modification of Newmark's method. Int J Numer Methods Eng 1980;15:1562–6.
[8] Kuhl D, Crisfield MA. Energy-conserving and decaying algorithms in non-linear structural dynamics. Int J Numer Methods Eng 1999;45(5):569–99.
[9] Bathe KJ, Noh G. Insight into an implicit time integration scheme for structural dynamics. Comput Struct 2012;98:1–6.
[10] Krieg RD. Unconditional stability in numerical time integration methods. J Appl Mech 1973;40:417–21.
[11] Tamma KK, Zhou X, Sha D. The time dimension: a theory towards the evolution, classification, characterization and design of computational algorithms for transient/dynamic applications. Arch Comput Methods Eng 2000;7:67–290.
[12] Butcher JC. Numerical methods for ordinary differential equations. Ltd, Chichester: John Wiley & Sons; 2016.
[13] Hilber HM, Hughes TJR. Collocation, dissipation and [overshoot] for time integration schemes in structural dynamics. Earthq Eng Struct Dyn 1978;6:99–117.
[14] Bazzi G, Anderheggen E. The ρ-family of algorithms for time-step integration with improved numerical dissipation. Earthq Eng Struct Dyn 1982;10:537–50. 12.
[15] Hoff C, Pahl PJ. Development of an implicit method with numerical dissipation from a generalized single-step algorithm for structural dynamics. Comput Methods Appl Mech Eng 1988;67:367–85.
[16] Zhou X, Tamma KK. Design, analysis, and synthesis of generalized single step single solve and optimal algorithms for structural dynamics. Int J Numer Methods Eng 2004;59:597–668.
[17] Noh G, Bathe KJ. Further insights into an implicit time integration scheme for structural dynamics. Comput Struct 2018;202:15–24.

[18] Maxam DJ, Tamma KK. A re-evaluation of overshooting in time integration schemes: The neglected effect of physical damping in the starting procedure. Int J Numer Methods Eng 2022:1–22. https://doi.org/10.1002/nme.695.
[19] Choi B, Bathe KJ, Noh G. Time Splitting ratio in the ρ_∞-Bathe time integration method for higher-order accuracy in structural dynamics and heat transfer. Comput Struct 2022;270:106814.
[20] Noh G, Bathe KJ. The Bathe time integration method with controllable spectral radius: the ρ_∞-Bathe method. Comput Struct 2019;212:299–310.
[21] Noh G, Bathe KJ. For direct time integrations: a comparison of the Newmark and ρ_∞-Bathe schemes. Comput Struct 2019;225:106079.
[22] Dvorkin EN, Bathe KJ. A continuum mechanics based four-node shell element for general non-linear analysis. Eng Comput 1984;1(1):77–88.
[23] Bathe KJ, Baig MMI. On a composite implicit time integration procedure for nonlinear dynamics. Comput Struct 2005;83(31-32):2513–4.
[24] Bathe KJ. Conserving energy and momentum in nonlinear dynamics: a simple implicit time integration scheme. Comput Struct 2007;85(7-8):437–45.
[25] Kwon SB, Bathe KJ, Noh G. Selecting the load at the intermediate time point of the ρ_∞-Bathe time integration scheme. Comput Struct 2021;254:106559.
[26] Noh G, Bathe KJ. An explicit time integration scheme for the analysis of wave propagations. Comput Struct 2013;129:178–93.
[27] Noh G, Ham S, Bathe KJ. Performance of an implicit time integration scheme in the analysis of wave propagations. Comput Struct 2013;123:93–105.
[28] Kwon SB, Bathe KJ, Noh G. An analysis of implicit time integration schemes for wave propagations. Comput Struct 2020;230:106188.
[29] Zakian P, Bathe KJ. Transient wave propagations with the Noh-Bathe scheme and the spectral element method. Comput Struct 2021;254:106531.
[30] Zhang H, Zhang R, Xing Y, Masarati P. On the optimization of n-sub-step composite time integration methods. Nonlinear Dyn 2020;102(3):1939–62.
[31] Zhang H, Zhang R, Masarati P. Improved second-order unconditionally stable schemes of linear multi-step and equivalent single-step integration methods. Comput Mech 2021;67(1):289–313.
[32] Wang Y, Tamma K, Maxam D, Xue T, Qin G. An overview of high-order implicit algorithms for first-/second-order systems and novel explicit algorithm designs for first-order system representations. Arch Comput Methods Eng 2021;28(5):3593–619.
[33] Wen W, Deng S, Wang N, Duan S, Fang D. An improved sub-step time-marching procedure for linear and nonlinear dynamics with high-order accuracy and high-efficient energy conservation. Appl Math Model 2021;90:78–100.
[34] Soares Jr D. A novel single-step explicit time-marching procedure with improved dissipative, dispersive and stability properties. Comput Methods Appl Mech Eng 2021;386:114077.
[35] Wen W, Deng S, Liu T, Duan S, Huang F. An improved quartic B-spline based explicit time integration algorithm for structural dynamics. Eur J Mech A Solids 2022;91:104407.
[36] Li J, Zhao R, Yu K, Li X. Directly self-starting higher-order implicit integration algorithms with flexible dissipation control for structural dynamics. Comput Methods Appl Mech Eng 2022;389:114274.
[37] Song C, Eisenträger S, Zhang X. High-order implicit time integration scheme based on Padé expansions. Comput Methods Appl Mech Eng 2022;390:114436.
[38] Li J, Yu K, Zhao R. Two third-order explicit integration algorithms with controllable numerical dissipation for second-order nonlinear dynamics. Comput Methods Appl Mech Eng 2022;395:114945.
[39] Ji Y, Xing Y. A two-step time integration method with desirable stability for nonlinear structural dynamics. Eur J Mech A Solids 2022;94:104582.
[40] Kim KT, Bathe KJ. Accurate solution of wave propagation problems. Comput Struct 2021;249.